WATER RESEARCH 44 (2010) 4359–4370

Available at www.sciencedirect.com

ScienceDirect

journal homepage: www.elsevier.com/locate/watres

Microbial community distribution and activity dynamics of granular biomass in a CANON reactor

Jose Vázquez-Padín [a,*], Anuska Mosquera-Corral [a], Jose Luis Campos [a], Ramón Méndez [a], Niels Peter Revsbech [b]

[a] Department of Chemical Engineering, University of Santiago de Compostela, Lope Gómez de Marzoa, s/n, E-15782, Spain
[b] Department of Microbiology, University of Aarhus, Ny Munkegade, Bldg. 540, 8000 Aarhus C, Denmark

ARTICLE INFO

Article history:
Received 23 October 2009
Received in revised form
14 May 2010
Accepted 27 May 2010
Available online 4 June 2010

Keywords:
Anammox
CANON
Granule
Autotrophic nitrogen removal
Microbial community
Microscale distribution

ABSTRACT

The application of microelectrodes to measure oxygen and nitrite concentrations inside granules operated at 20 °C in a CANON (Complete Autotrophic Nitrogen-removal Over Nitrite) reactor and the application of the FISH (Fluorescent In Situ Hybridization) technique to cryosectioned slices of these granules showed the presence of two differentiated zones inside of them: an external nitrification zone and an internal anammox zone. The FISH analysis of these layers allowed the identification of *Nitrosomonas* spp. and *Candidatus* Kuenenia Stutgartiensis as the main populations carrying out aerobic and anaerobic ammonia oxidation, respectively.

Concentration microprofiles measured at different oxygen concentrations in the bulk liquid (from 1.5 to 35.2 mg O_2 L^{-1}) revealed that oxygen was consumed in a surface layer of 100–350 μm width. The obtained consumption rate of the most active layers was of 80 g O_2 $(L_{granule})^{-1}$ d^{-1}. Anammox activity was registered between 400 and 1000 μm depth inside the granules. The nitrogen removal capacity of the studied sequencing batch reactor containing the granular biomass was of 0.5 g N L^{-1} d^{-1}. This value is similar to the mean nitrogen removal rate obtained from calculations based on in- and outflow concentrations. Information obtained in the present work allowed the establishment of a simple control strategy based on the measurements of NH_4^+ and NO_2^- in the bulk liquid and acting over the dissolved oxygen concentration in the bulk liquid and the hydraulic retention time of the reactor.

1. Introduction

Efficient nutrients removal from wastewater is essential due to disposal legislation demanding stricter effluent concentrations. Nitrogen removal from wastewaters characterized by low organic matter content and high nitrogen concentrations is difficult by the application of conventional processes like nitrification-denitrification. In these cases, the anammox process arose as an interesting alternative since the anammox bacteria oxidize ammonium anaerobically with nitrite as electron acceptor in the absence of organic carbon compounds. Prior to the anammox reaction, part of the ammonium has to be oxidized into nitrite. This step can be carried out separately in different kind of reactors, e.g., a Sharon (Single reactor system for High activity Ammonium Removal Over Nitrite) reactor (van Dongen et al., 2001; Mosquera-Corral et al., 2005), a granular nitrifying reactor (Vázquez-Padín et al., 2009), etc. Another possibility is to

* *Corresponding author*. Tel.: +34 981 563100x16739; fax: +34 981 528050.
E-mail address: jose.vazquez.padin@usc.es (J. Vázquez-Padín).
0043-1354/$ – see front matter © 2010 Elsevier Ltd. All rights reserved.
doi:10.1016/j.watres.2010.05.041

perform the partial nitrification and the anammox processes in one single reactor. This process has been given different names: CANON (Complete Autotrophic Nitrogen-removal Over Nitrite; Third et al., 2001), OLAND (Oxygen Limited Autotrophic Nitrification-Denitrification; Kuai and Verstraete, 1998) and deammonification (Hippen et al., 1997) processes. Under microaerobic conditions, ammonia oxidizing bacteria (AOB) oxidize ammonium into nitrite consuming the dissolved oxygen (DO) and creating anoxic niches where anammox bacteria can exist and convert both ammonia and nitrite into nitrogen gas and produce small amounts of nitrate. The optimization of the performance of the autotrophic nitrogen removal in the CANON process requires the control of dissolved oxygen (DO) and NO_2^- concentrations. To establish an adequate control of the DO concentration in the liquid media is necessary: 1) to avoid the inhibition of anammox bacteria caused by DO concentrations higher than 0.5% of air saturation (Strous et al., 1997), 2) to prevent the growth of nitrite oxidizing bacteria (NOB) which have lower affinity for oxygen compared to AOB. The control of NO_2^- concentration is necessary since this compound inhibits anammox activity although variable ranges of concentrations are provided in the literature for this inhibitory effect. Dapena-Mora et al. (2007) reported that concentrations of nitrite of 350 mg NO_2^-–N L^{-1} resulted in 50% inhibition of anammox bacteria.

Due to the slow growth of both nitrifying and anammox bacteria involved in the CANON process, the use of good biomass retention systems is mandatory to reach significant nitrogen removal rates. In this sense, the development of granular biomass allows the accumulation of large biomass concentrations in the reactors without the need of carrier material. Moreover, the use of granular biomass allows the existence of substrate gradients, in such a way that the external part of granule can be under aerobic conditions while anoxic conditions are maintained in the core of the granule. Therefore, different biological processes can be carried out in the same granule: partial nitrification in the outer part and anammox in the inner part. The potential of the technologies based on single-reactors to carry out autotrophic nitrogen removal using granular biomass has been demonstrated (Vlaeminck et al., 2008; Vázquez-Padín et al., 2009). Using these systems it is possible to treat nitrogen loads similar to systems with two different units for partial nitrification and anammox processes, respectively.

Microsensors, due to their very small dimensions, can be used for the determination of substrate profiles while the distribution of bacterial populations can be determined by microbiological techniques (e.g. FISH, PCR). The combination of microbiological techniques and measurements using microelectrodes has previously been used to obtain detailed knowledge about the in situ structure and function of nitrifying biofilms. Schramm et al. (1999) and Kindaichi et al. (2006) used this combination to estimate kinetic parameters to be further used in mathematical models. de Beer et al. (1993) and Gieseke et al. (2003) studied the mass transport of substrates through biofilms or aggregates using microelectrodes and determined the limiting substrate, the size of the active zone of the biofilm and the biomass activities under different substrate concentrations. These techniques are also suitable for the determination of the spatial distribution of substrate consumption rates in non- homogeneous biofilm reactors (Schramm et al., 1999; Kindaichi et al., 2007), for researching the environmental conditions (e.g., pH) inside the biofilm (Gieseke et al., 2006) or for observing the stratification of active biomass (Okabe et al., 1999; Kindaichi et al., 2006).

The combination of microsensor measurements and FISH analysis makes it possible to gain information about the substrate concentrations to which the different layers of a biofilm/aggregate are exposed and about the microbial populations involved in the different biological processes. All the microscopic information could then be transposed to a macroscopic level, giving valuable information about the possible control strategies of CANON reactors.

Since little information is known from a microscopic point of view about granules performing complete autotrophic nitrogen removal and taking into account the relevance of DO and NO_2^- concentrations, the objectives of this study were: the identification of the main bacteria populations present in the granules, the determination of their distribution inside the granules and the estimation of their activities by combining the concentrations profiles measured with microelectrodes and FISH images taken from cryosectioned slices of granules. The improved insight into the functioning of the CANON aggregates should then be used to devise a control strategy for the optimization of the reactor performance.

2. Materials and methods

2.1. *Reactor description*

The growth of biomass in the form of granules performing the CANON process was described elsewhere (Vázquez-Padín et al., 2009). Initially, the complete nitrification was developed and later, after the regulation of the DO concentration in the bulk liquid, the partial nitrification to nitrite was achieved. Finally, anammox bacteria were grown in the anoxic core of the granules to form the CANON granules.

Five months after the appearance of the macroscopic evidence of anammox activity in the CANON granules, 4 g VSS of granular biomass from an anammox reactor operated at the University of Santiago de Compostela were inoculated into a sequencing batch reactor (SBR) with a working volume of 0.7 L at the University of Aarhus. This new reactor was operated in cycles of 3 h distributed as: 175 min of aeration and feeding, 1 min of settling and 4 min for effluent withdrawal. The hydraulic retention time (HRT) was fixed at 0.45 d and the exchange volume was fixed at 30%.

The reactor was operated at room temperature which ranged between 19 and 22 °C. The pH value was not controlled and ranged from 7.0 to 8.1 with a mean value of 7.6. Air was supplied through a diffuser at the bottom of the reactor to promote the transfer of oxygen into the bulk liquid and to reach a suitable mixing. The average DO concentration in the reactor was 6.6 mg O_2 L^{-1} and this represented the main difference as compared to the operational conditions of the reactor operated at the laboratory in Santiago de Compostela where the DO was kept around 3.5 mg O_2 L^{-1}.

The CANON SBR was fed with the supernatant from the anaerobic sludge digester of the WWTP of Aarhus (Denmark)

which was stored in a cold room (4 °C). The main properties of the supernatant were: pH of 7.6–8.3; ammonium concentration of 256–666 mg N L^{-1}; inorganic carbon (IC) of 232–374 mg IC L^{-1} and total organic carbon (TOC) of 103–150 mg TOC L^{-1} which was poorly biodegradable.

2.2. k_La measurement

An experimental estimation of the oxygen gas-liquid transfer coefficient (k_La) was carried out by means of a dynamic method, registering the increments of DO concentrations in the SBR after the reestablishment of the aeration (without biomass in the reactor). The value of the k_La for dissolved oxygen obtained in the reactor was of 1 min^{-1} which was similar value to the value obtained in the case of the SBR installed in Santiago de Compostela.

2.3. Microscale experiments

Microsensors were used to measure the concentration profiles of nitrite and dissolved oxygen (DO) inside the granules performing the CANON process. The granules were collected directly from the CANON SBR and fastened with a needle to a metal grid inside the experimental chamber. In order to simulate the hydrodynamic conditions from the reactor, the aeration flow in the chamber was regulated to maintain a k_La value of 1 min^{-1} which was the same value as in the SBR. All the microprofiles were measured in granules with average diameters of 5 mm. The mean temperature of the aerated chamber was 20 ± 1 °C. Granules were kept for 1 h inside the chamber as a pre-incubation period to create pseudo steady state conditions. Concentration profiles were recorded by introducing the sensors into the granules at different depth positions using a manual micromanipulator. A dissection microscope was used to visually estimate the position of the granule/water interface by visual observation. For each granule and experimental condition tested several microprofiles were measured (the number of microprofiles performed is indicated in the caption of figures as *n*). Microprofiles of DO were performed by measuring its concentration at depth intervals of 25 μm while in the case of the microprofiles of NO_2^- the measurements were performed at 50 or 100 μm intervals due to a slower response time of this sensor. The sensor signal was continuously recorded on a strip-chart recorder.

The liquid medium inside the chamber was the anaerobic digester supernatant diluted with tap water. The concentration of ammonium was in all experiments maintained constant at 140 mg N L^{-1} in order to avoid ammonium limitation. The nitrite concentrations were varied from 0.7 to 42 mg NO_2^-–N L^{-1} by $NaNO_2$ addition. The microsensors were calibrated prior to each experiment using the same basic medium with various added nitrite concentrations.

The dissolved oxygen concentration in the bulk liquid was varied between 1.5 and 35.2 mg O_2 L^{-1}. These different DO concentrations were achieved by flushing a mixture of pure O_2 and air for DO values in the aeration chamber above air saturation, or a mixture of air and N_2 for DO values under air saturation. In order to maintain a constant k_La, in all the experiments the total gas flow (N_2/air/O_2) was kept constant.

2.4. NO_2^- and O_2 microsensors

Microsensors were used to determine concentrations of the measured compounds inside the granules.

A Clark-type O_2 microsensor equipped with a guard cathode was used for microscale analysis of DO (Revsbech, 1989). The sensor was made with a tip diameter of 10 μm and it had a 90% response time lower than 2 s. The oxygen microsensor was calibrated at two concentration points: the zero value was established by inserting the microsensor into an anoxic alkaline ascorbic acid solution and the other calibration point was obtained by means of an air saturated solution or a pure oxygen saturated solution, depending on the DO range to be tested.

The NO_2^- microsensor was a biosensor containing an immobilized pure culture of *Stenotrophomonas nitritireducens* that reduced NO_2^-–N_2O, which was quantified by a built-in Clark-type N_2O microsensor (Nielsen et al., 2005). The 90% response time was 30–50 s. Due to the broad range of NO_2^- concentrations in the bulk liquid varying from 0.7 to 42 mg NO_2^-–N L^{-1} it was necessary to use Electrophoretic Sensitivity Control (ESC) to adjust the sensitivity of the sensor to the relevant concentration range (Kjær et al., 1999).

2.5. Analytical methods

The pH and the concentrations of DO, ammonium, nitrite, nitrate, volatile suspended solids (VSS), settling velocity and sludge volumetric index (SVI) were determined according to the Standard Methods (APHA-AWWA-WPCF, 1998). Concentrations of TOC and IC were measured with a Shimadzu analyser (TOC-5000). Density of the granules was measured using the dextran blue method described by Beun et al. (2001). The morphology and size distribution of the granules were measured regularly by using an image analysis procedure with a stereomicroscope (Stemi 2000-C, Zeiss) provided with a digital camera (Coolsnap, Roper Sicientific Photometrics). For the digital image analysis the programme Image Pro Plus was used.

2.6. Description of the FISH protocol

In order to identify bacterial populations of AOB, NOB and anammox bacteria, granules from the reactor were collected, kept in their aggregated form or disaggregated, and fixed according to Amann et al. (1995) with 4% paraformaldehyde solution. Entire granules were embedded in OCT reagent (Tissue-Tek; Miles, Ind.) prior to their cryosectioning at −35 °C. Slides with a thickness of 14 μm were cut at −16 °C and each single section was placed on the surface of poly-L-lysine coated microscope slides. Hybridization was performed at 46 °C for 90 minutes adjusting formamide concentrations at the percentages shown in Table 1. The used probes for in situ hybridization were 5′ labelled with the fluorochromes FITC, Cy3 or Cy5. A TCS-SP2 confocal laser scanning microscope (Leica, Germany), equipped with a HeNe laser for detection of Cy3 and Cy5 and one Ar ion laser for detection of FITC, was used with the sliced samples.

The method to quantify bacterial populations was based on the one published by Crocetti et al. (2002). The digital image

Table 1 – Targeted organisms and the corresponding formamide (FA) percentages for the used oligonucleotide probes.

Probe[a]	Probe sequence (5′→3′)	% FA	Targeted organisms
EUB338	GCT GCC TCC CGT AGG AGT	0–50	Domain *bacteria*
EUB338 II	GCA GCC ACC CGT AGG TGT	0–50	Planctomycetales
EUB338 III	GCT GCC ACC CGT AGG TGT	0–50	Verrucomicrobiales
Nso190	CGA TCC CCT GCT TTT CTC C	55	Ammonia-oxidizing β-*Proteobacteria*
NEU653[b]	CCC CTC TGC TGC ACT CTA	40	Most of the halophilic and halotolerant *Nitrosomonas* spp.
Ntspa712[b]	CGC CTT CGC CAC CGG CCT TCC	50	Most members of the phylum *Nitrospira*
NIT3[b]	CCT GTG CTC CAT GCT CCG	40	*Nitrobacter* spp.
AMX820	AAA ACC CCT CTA CTT AGT GCC C	40	Anaerobic ammonium-oxidizing bacteria *Candidatus* Brocadia anammoxidans and *Candidatus* Kuenenia stuttgartiensis
Kst157	GTT CCG ATT GCT CGA AAC	25	*Candidatus* Kuenenia stuttgartiensis
Ban162	CGG TAG CCC CAA TTG CTT	40	*Candidatus* Brocadia anammoxidans

a Details on oligonucleotide probes are available at probeBase (Loy et al., 2007).
b Used with an equimolar amount of corresponding unlabeled competitor oligonucleotide probe.

analysis program used was Image ProPlus®. For the quantification of bacteria populations, cryosectioned slices of granules were used to perform a triple hybridization with EUBmix (a mixture of EUB338, EUB338 II and EUB338 III) labelled with Cy5, AMx820 labelled with Cy3 and NEU653 labelled with FITC. Several pictures were taken subsequently from the granule surface throughout the active layers with the confocal microscope at a magnification of 630 times. From each image three different colour components corresponding to each fluorochrome were separated generating three different images. The area corresponding to the fluorescence of each FISH probe was obtained as the area of all pixels above one value manually determined corresponding to the minimum pixel intensity. In order to be able to compare the areas occupied by the different populations, the maximal area occupied in a discretized picture was taken as reference and the values of fluorescence obtained with the different probes in the different layers were obtained as normalized area values.

3. Calculations

3.1. *Estimation of oxygen and nitrite consumption and production rates*

Dissolved oxygen and nitrite mass balances were calculated for the granules using a one-dimensional diffusion model. The activities of the nitrogen removal processes occurring inside the granules were restricted to an external layer of 1 mm (as it will be further discussed) which was smaller than the mean radius of the granules used to record the microprofiles (mean radius of 2.5 mm).

In this calculation procedure the assumption was made that the diffusional transport into the granules can be modelled as a one-dimensional transport, as the diameter of granules was large (5 mm) compared to the studied surface layer (1 mm). The concentration changes with time for a diffusible substance in a matrix with a flat geometry can be written according to Eq. 1. It is assumed that the compound mass transfer is carried out only by diffusion and that the granule has a homogeneous structure so that the diffusion coefficient (D) can be considered constant (Lorenzen et al., 1998).

$$\frac{\partial C(z,t)}{\partial t} = D\,\frac{\partial^2 C(z,t)}{\partial z^2} + A(z) \tag{1}$$

where C is the concentration of the compound (g L^{-1}), z the depth coordinate in the granule (dm), t the time (d) and A the reaction rate (g $(L_{granule})^{-1}$ d^{-1}). Assuming steady state conditions Eq. 2 is obtained.

$$D\,\frac{\partial^2 C(z)}{\partial z^2} = -A(z) \tag{2}$$

using Euler's formula for numeric integration, Eq. 3 is obtained.

$$\frac{\partial C}{\partial z_{n+1}} = \frac{\partial C}{\partial z_n} + h\,\frac{A_n}{D} \tag{3}$$

where h represents the step size used for numerical integration. This discretization parameter was of 25 μm for the oxygen profiles and of 50 μm for nitrite profiles with concentrations in the bulk liquid smaller than 2.8 mg NO_2^-–N L^{-1} and of 100 μm for higher NO_2^- concentrations. After further integration Eq. 4 is obtained.

$$C_{n+1} = C_n + h\,\frac{\partial C}{\partial z_n} \tag{4}$$

Substituting Eq. 3 in Eq. 4, Eq. 5 is obtained.

$$C_{n+1} = C_n + h\,\left(\frac{\partial C}{\partial z_{n-1}} + h\,\frac{A_{n-1}}{D}\right) \tag{5}$$

Using the Solver tool (available in Microsoft Excel® software) the values of A (i.e., the local volumetric consumption rate) were iterated in order to minimize the error between the concentration calculated with Eq. 2 and that one measured with the microsensor. The values of the diffusion coefficients of NO_2^- and O_2 in water at 20 °C were chosen as 1.5×10^{-4} and 1.7×10^{-4} m^2 d^{-1}, respectively (Picioreanu et al., 1997).

To calculate the fluxes of substrates (J, g N m^{-2} d^{-1}) through the diffusive boundary layer (DBL) which separates the surface of the granule and the bulk liquid, Fick's first law of diffusion was used (Eq. 6).

$$J = -D_W\frac{C_b - C_s}{\delta_h} \tag{6}$$

being D_w the molecular diffusion coefficient in water (m^2 d^{-1}), C_b is the bulk liquid concentration (g m^{-3}), C_S is the concentration (g m^{-3}) at the surface of the granule, and δ_h is the

hypothetical (also called effective) thickness of the diffusive boundary layer (m) which is defined by extrapolating the radial oxygen gradient at the granule-water interface to the bulk water phase concentration (Ploug et al., 1997).

3.2. Nitrogen removal rates

Ammonia oxidation rates (AOR) and nitrogen removal rates by anammox bacteria (ANR) of the CANON granular reactor were estimated as g N L^{-1} d^{-1} based on nitrogen balances and the stoichiometry of the anammox process (1.02 moles of dinitrogen gas produced per mole of ammonium reacted).

$$\Delta N = \left(NH_4^+ - N_{inf}\right) - \left(\left(NH_4^+ - N_{eff}\right) + \left(NO_2^- - N_{eff}\right) + \left(NO_3^- - N_{eff}\right)\right) \quad (7)$$

$$AOR = \frac{\left(NH_4^+ - N_{inf}\right) - \left(NH_4^+ - N_{eff}\right) - \frac{\Delta N}{2.04}}{HRT} \quad (8)$$

$$ANR = \frac{\Delta N}{HRT} \quad (9)$$

Where ΔN is the difference between total nitrogen concentration in the influent and effluent (g N L^{-1}), NH_4^+–N_{inf} is the ammonium concentration in the influent (g N L^{-1}) and NH_4^+–N_{eff}, NO_2^-–N_{eff}, NO_3^-–N_{eff} are the ammonium, nitrite and nitrate concentrations in the effluent (g N L^{-1}), respectively.

3.3. Estimation of the number of granules

The number of granules in the reactor was calculated as follows:

$$V_{granule} = \frac{V_R \cdot X_R}{\rho_{granule}} \quad (10)$$

$$n_T = \frac{V_{granule}}{\frac{4}{3} \cdot \pi \cdot R_m^3} \quad (11)$$

Where $V_{granule}$ is the volume of granules (L), V_R is the reactor volume (L), X_R is the biomass concentration in the reactor (g VSS L^{-1}), $\rho_{granule}$ is the granules density (g VSS $(L_{granule})^{-1}$), n_T is the number of granules, and R_m is the average radius of the granules (dm).

In order to estimate either the AOR or the ANR from the microscopic observations, Eq. 12 was used to describe the zone were AOB or anammox bacteria were located.

$$Rate = \frac{n_T \cdot \sum_{z=1}^{n} \left(A(z) \cdot \frac{4}{3} \cdot \pi \cdot \left(R_z^3 - R_{z-1}^3\right)\right)}{V_R} \quad (12)$$

Where the rate is calculated in terms of g $(L_{reactor})^{-1}$ d^{-1}, A is the local reaction rate (g $(L_{granule})^{-1}$ d^{-1}), V_R is the reactor volume (L), and r corresponds to the granule radius (dm).

4. Results and discussion

4.1. Operation of the CANON SBR

The SBR reactor was operated at DO concentrations around 6.6 mg O_2 L^{-1} and at a temperature of 20 °C. The mean NO_2^- concentration in the effluent was 25 mg N L^{-1}. The total nitrogen removal rate (Fig. 1) ranged between 0.35 and 0.91 g N L^{-1} d^{-1}. Those values are among the highest ones registered for autotrophic nitrogen removal in one reactor despite the low temperature of operation. According to Dosta et al. (2008) there is a strong dependence between the temperature and the anammox activity in such a way that the specific activity of anammox biomass at 37 °C is 3.6 times higher than at 20 °C.

The biomass concentration inside the reactor remained almost constant at 7.5 g VSS L^{-1} during the 60 days of operation. The average diameter and density of the granules were 5 mm and 36 g VSS $(L_{granule})^{-1}$, respectively. With these data, the number of granules was estimated, using Eq. 11, as 2230 granules. The value of the SVI was 25 mL (g VSS)$^{-1}$ and the settling velocity of the granular sludge was of 110 m h^{-1}.

4.2. Identification of bacteria populations by FISH

The stratification of the AOB and anammox bacteria in depth inside the granule can be observed in Fig. 2. In the outermost 200 μm layer of the granule almost all the biomass consisted of *Nitrosomonas* spp. which gave positive signals to probes NEU653 and Nso190. Bacteria belonging to the genus *Nitrosomonas* spp. were still present at a depth of 600 μm but their proportion decreased when the depth increased (Fig. 2). *Nitrosomonas* spp. was identified as the main AOB community as it was expected due to operational conditions in the reactor with ammonium concentration in excess (Schramm et al., 1998).

Significant fluorescence signal was detected neither with probe NIT3 specific for *Nitrobacter* spp. nor with probe Ntspa712 specific for the *Nitrospira* phylum. Therefore, no NOB activity was expected in the granules despite the high DO concentration in the liquid bulk.

Anammox bacteria were mainly located between 400 and 1000 μm in depth inside the granule where dissolved oxygen was absent during normal reactor operation. Bacteria belonging to the genus *Candidatus* Kuenenia stuttgartiensis were identified as the main anammox bacteria in the reactor through positive results with probe Kst157. No positive results with probe Ban162 were obtained indicating absence of *Candidatus* Brocardia anammoxidans. Thus, in the depth interval between 400 and 600 μm the AOB and anammox bacteria coexisted.

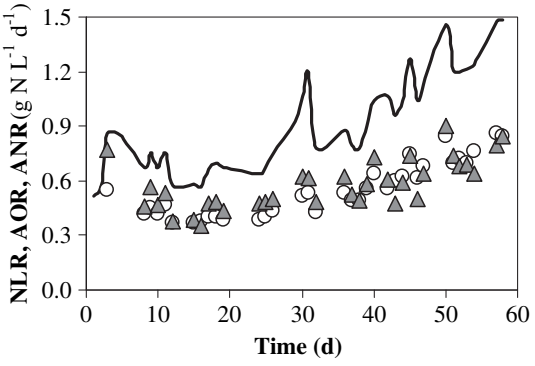

Fig. 1 – Applied nitrogen loading rate (–), ammonia oxidation rate (○), nitrogen removal rate (△).

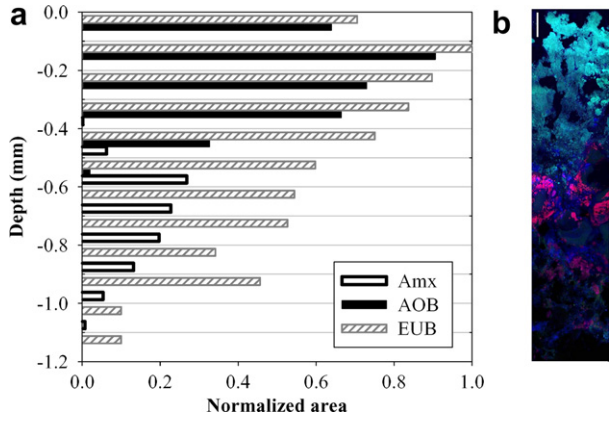

Fig. 2 – a) Depth distribution of AOB populations (hybridized with probe NEU653), anammox bacteria (hybridized with probe AMX820) and all bacteria (hybridized with EUBmix) inside the granule. The value of depth equal to 0 mm corresponds to the granule surface. b) Image of a cryosectioned slice of a granule with a triple hybridization of FISH probes targeting: AOB (probe: NEU653; fluorochrome: FITC; colour: light green); anammox bacteria (probe: AMX820; fluorochrome: Cy3; colour: pink) and all bacteria (probe: EUBmix; fluorochrome: Cy5; colour: blue). The right part of the picture corresponds to the surface of the granule (the bar corresponds to 75 μm).

It is also interesting to point out that the area corresponding to EUBmix probe which represent all bacteria decreased with the increase in depth inside the granule and that the activity was mainly located in the external 1000 μm of the granule.

4.3. *Microprofiles measurements*

4.3.1. *Oxygen microprofiles in the partial nitrification zone*

In order to determine the oxygen consumption kinetics, microprofiles were measured along the granule varying the DO concentration in the bulk liquid over a wide range, from 1.5 to 35.2 mg O_2 L^{-1} (Fig. 3) with an initial ammonium concentration of 140 mg N L^{-1}.

The trend of the concentration profiles was similar in all cases illustrating the various steps of oxygen transport and consumption: first the diffusion of DO through the external diffusive boundary layer (DBL) and later the internal diffusion together with the biological reaction which resulted in a curve profile. The external mass transfer resistance was significant as a large decrease of DO concentration could be observed between the bulk liquid and the granule surface. This significant decrease of DO concentration within the DBL working with highly active biofilms has also been reported by other authors (Jørgensen and Revsbech, 1985; de Beer et al., 1993; Rasmussen and Lewandowski, 1998; Wilen et al., 2004). This demonstrates that the external mass transfer resistance plays an important role specially when working with granules with a mean diameter of 5 mm. In the present study the width of the external DBL was around 100–120 μm.

Regarding the DO microprofiles inside the granules, it was observed that the oxygen penetration depth increased from 100 to 350 μm when increasing the DO in the bulk liquid from 1.5 to 35.2 mg O_2 L^{-1} (Fig. 3). The microprofiles revealed that even when the DO concentration in the bulk liquid was kept at 8 mg O_2 L^{-1} (close to 100% of air saturation), the maximal oxygen consumption rate was only attained in the outer part of the granule (corresponding to a depth of around 30 μm). Moreover, a fast decrease in the DO concentration in depth inside the granule was registered in all the cases demonstrating that the oxygen mass transfer rate strongly limited the ammonia oxidation process. The high oxygen demand in the surface layer allowed an anoxic zone to be created in the internal part of the granule where the anammox process could take place.

An estimation of the affinity constant of the AOB was performed using the profiles obtained with the highest DO concentrations in the bulk liquid. The value obtained was 0.6 mg O_2 L^{-1}, which is in agreement with the values previously published for AOB at 20 °C (Wiesmann, 1994; Guisasola et al., 2005).

According to Harremoes and Henze (2002) the reaction rate can be modelled as a function of the concentration of substrate outside a biofilm using 3 kinetic orders: 1; 1/2 and 0. A kinetic order of 1 is a good approximation when the substrate concentrations in the bulk liquid are lower than $2 \cdot K_S$ (K_S is the half saturation constant for the substrate S), and a kinetic order of 0 is obtained when the biofilm is fully penetrated by the substrate (assuming a low K_m value). Half order kinetics represents the transition between 1 and 0 order and it is caused by the progressively deeper substrate penetration into the biofilm with the increasing bulk concentration. In Fig. 4, the AOR is represented versus the square root of DO concentration at the surface of the granules. The AOR in the SBR was estimated using Eq. 12 considering the stoichiometry requirements for ammonium oxidation: 3.4 g O_2 (g NH_4^+–N)$^{-1}$. As it was expected according to Harremoes and Henze (2002), the tendency of these values is linear, i.e. 1/2 order kinetic, and even when working with pure oxygen in the bulk liquid, the granule was oxygen limited. Wilen et al. (2004) estimated that the DO required to obtain a 0 order kinetic was higher than 20 mg O_2 L^{-1} in aggregates with a diameter of 0.50–0.69 mm, and it is then expected that the experiments performed with much larger aggregates exhibited half order kinetics These results illustrate the key role of the mass transfer limitations on the overall biomass activity of the granular sludge.

The reactor was usually operated at DO concentrations of 6.6 mg O_2 L^{-1} meaning that the oxygen is available only in the first 200 μm of the granule. When the DO concentration in the bulk liquid was increased up to pure DO saturation, progressively deeper layers became active which indicates that nitrifying bacteria might be able to remain alive in the absence of substrates and very quickly be activated as soon as NH_4^+ and DO are supplied. Such long term survival of the nitrifying bacteria under ammonium-starving or anoxic conditions has previously been reported (Wilhelm et al., 1998; Freitag and Prosser, 2003).

Oxygen profiles along the nitrifying granules/biofilms reported in literature are shown in Table 2. The different

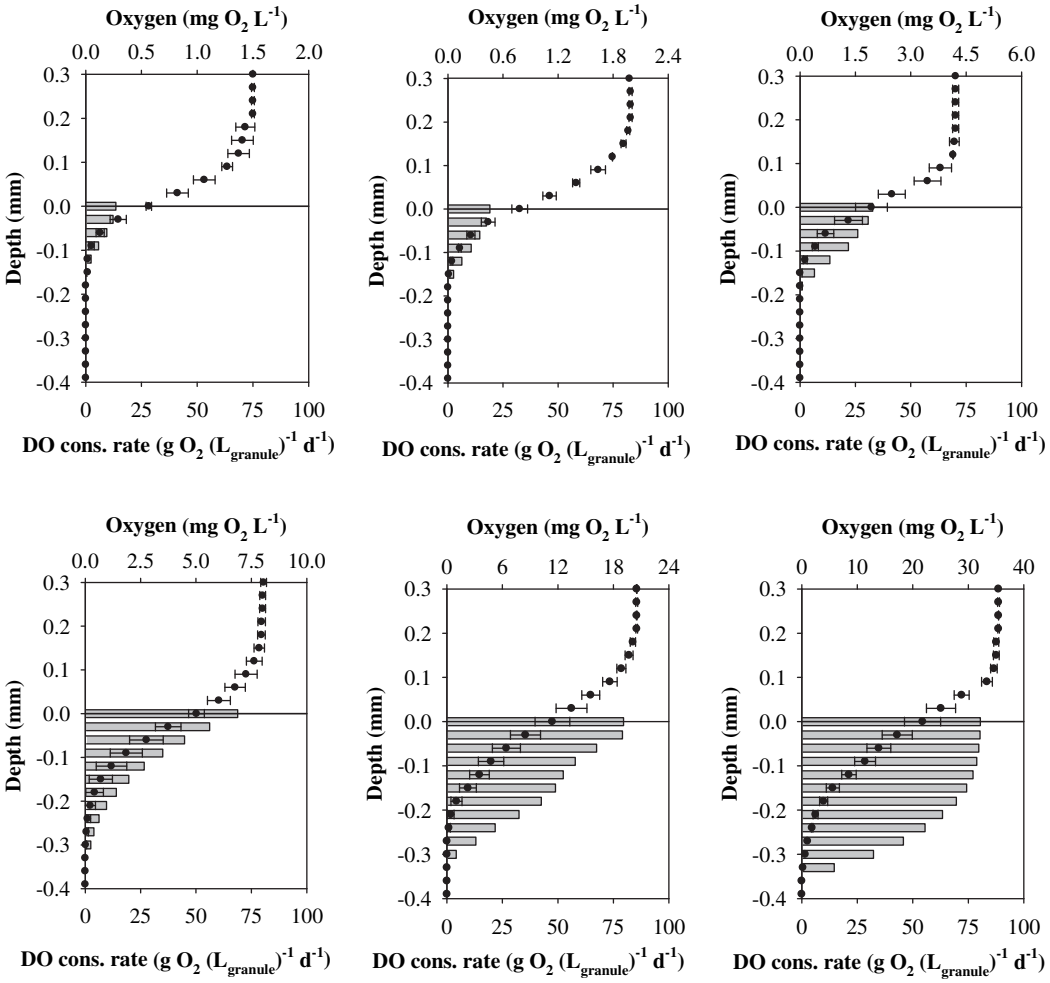

Fig. 3 – Dissolved oxygen concentration profiles (●, bars indicate standard deviation) and local consumption rates (▯) under different DO concentrations in the bulk liquid (number of microprofiles performed (*n*): $n = 3$ for all cases except for DO = 8 mg O_2 L^{-1} where $n = 20$). Note the different concentration scales.

biofilms or granules analyzed came from different reactors with different hydrodynamics characteristics: rotating disk reactors (Okabe et al., 1999; Kindaichi et al., 2006); fluidized bed reactors (de Beer et al., 1993; Schramm et al., 1999); sequencing batch biofilm reactor (Gieseke et al., 2003) and granular SBR (Wilen et al., 2004; this study). The thickness of the DBL ranged between 91 and 140 μm and a considerable DO drop through the diffusive boundary layer was always observed which shows the importance of the external mass transfer resistance. The nitrifying activity was mainly concentrated in the first 100 μm resulting in a steep gradient of DO concentration.

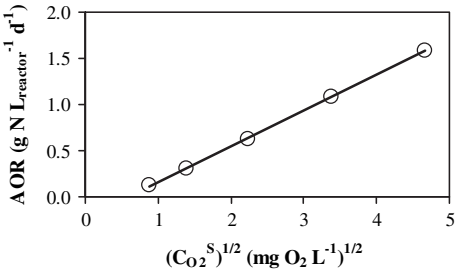

Fig. 4 – AOR estimation from oxygen microprofiles vs. square root of DO concentration at the surface of the granule (with trend line).

From the obtained values it can be inferred that the oxygen flux is mainly influenced by the DO in the bulk liquid and by the temperature of operation since this affects the biomass activity (Jubany et al., 2008).

4.3.2. *Nitrite microprofiles in the partial nitrification zone*

NO_2^- microprofiles were determined under conditions of excess of ammonium (initial NH_4^+ concentration in the bulk liquid was fixed at 140 mg N L^{-1}), starting with low concentration of nitrite in the bulk liquid and at different DO concentration. NO_2^- microprofiles corresponding to the three higher DO concentrations tested are represented in Fig. 5. Low NO_2^- concentrations in the bulk liquid were used in order to obtain a clearly visible nitrite peak in the nitrification zone allowing the calculation of the nitrification rate profiles. The NO_2^- concentration at the surface of the granules was

Table 2 – Comparison of DO microprofiles in autotrophic nitrifying biofilms.

DO_{bulk} (mg O_2 L^{-1})	$DO_{surface}$ (mg O_2 L^{-1})	$DO_{100\ \mu m}$ (mg O_2 L^{-1})	T (°C)	Biofilm width (μm)	DBL δ_h (μm)	J_{O_2} (g O_2 m^{-2} d^{-1})	Ref[d]
8.0	2.9	0.2	30	1000–1250[c]	120	10.5[a]	[1]
7.4	4.5	1.3	30	500–1500[c]	100[a]	10.6[a]	[2]
8.0	2.6	0.2	25	200–500	100	5.9[b]	[3]
7.4	3.7	1.3	20	200	140	5.0[a]	[4]
6.1	3.0	0.6	20	350	100	5.2	[5]
8.0	4.8	1.4	20	2500[c]	108	5.1	T.S.
2.0	0.5	0.0	25–27	400	91[a]	2.8[b]	[6]
2.0	0.8	0.1	20	2500[c]	120	1.8	T.S.

a Values published by the authors in the indicated reference. The value published by Kindaichi et al. (2006) was the ammonium flux of 1.1 g N m^{-2} d^{-1} and it was converted to oxygen flux with the stoichiometric coefficient (4.57 g O_2 per g NH_4^+–N for complete nitrification).
b Values estimated considering an oxygen diffusivity at 25 °C of 1.9 × 10^{-4} m^2 d^{-1} (Gieseke et al., 2003).
c Radius of the granules.
d [1] Schramm et al. (1999): Values corresponding to the port A of the fluidized bed reactor [2] de Beer et al. (1993) [3] Gieseke et al. (2003) [4] Kindaichi et al. (2006) [5] Okabe et al. (1999) [6] Wilen et al. (2004): Values corresponding to the upstream microprofile of the reference. T.S. = this study.

significantly higher than the NO_2^- concentration in the bulk liquid. Two well defined zones could be differentiated: 1) the nitrification zone, corresponding to the external layers in contact with the bulk liquid where nitrite was produced by AOB and 2) the anammox zone where NO_2^- was consumed together with NH_4^+ under anoxic conditions. From the obtained microprofiles it is observed that the nitrite peak and the nitrite production rate became higher by increasing the DO concentration in the bulk liquid. Due to the produced concentrations gradient in the nitrification zone, nitrite diffused to both bulk liquid and inner layers of the granule. These concentrations gradients were caused by the nitrite generation in the nitrifying zone, its diffusional transfer to the bulk liquid during continuous operation, and the NO_2^- consumption in the inner layers by anammox bacteria. However, the steepness of the NO_2^- gradient in the DBL is an artefact caused by the low NO_2^- concentration in the bulk liquid, and inside the reactor on the average there should be a considerably lower net flux to the liquid phase than that suggested by the present model example.

The zone of NO_2^- production determined with the NO_2^- microsensor fitted well with the one obtained using the DO microsensor. A lower level of details compared to the DO microprofiles was obtained due to the bigger discretization step used (50 μm instead of 25 μm) and the Monod kinetic was also well reflected with higher activities in the external layers. Similar as in the case of DO consumption, using pure DO saturation, the width of the outer 200 μm layer of the granules was working at maximal activity.

The oxygen consumption rates were five times higher than the nitrite production rates. This ratio is superior to the stoichiometrically required one (according to the stoichiometry of ammonia oxidation to nitrite, the ratio would be 3.4 g O_2 (g N)$^{-1}$). The different obtained values can be attributed to a mismatch of the NO_2^- diffusivity. The NO_2^- diffusivity might be enhanced/decreased by the production of anions and cations in the aggregate which would cause the diffusivity NO_2^-/diffusivity O_2 ratio in the nitrification zone to have a different value than the ratio in pure water. The diffusional transport of negative and positive ions through the aggregates

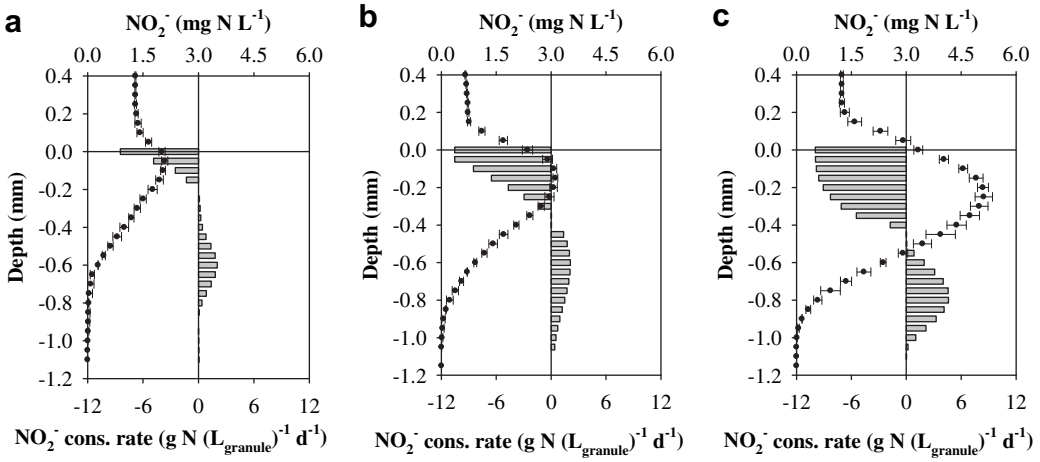

Fig. 5 – Nitrite profiles (●, bars indicate standard deviation, $n = 3$) and local consumption rates (bar) under different O_2 concentrations in the bulk liquid: a) DO = 8.0 mg O_2 L^{-1} b) DO = 20.5 mg O_2 L^{-1} c) DO = 35.2 mg O_2 L^{-1}. The NO_2^- concentration in the aqueous phase was kept at low values around 1 mg L^{-1}.

and the bulk liquid must be in equilibrium. This may affect the ion diffusivities which may be different from the self-diffusion coefficients (Reimer and Harremoes, 1978). In fact, the actual diffusion coefficients might even be more different than the ±10% suggested by literature (Li and Gregory, 1974; Picioreanu et al., 1997).

The flux of NO_2^- out of the nitrification zone, the total flux (i.e., the NO_2^- production), and the flux to the core of the granule are shown in Table 3. As it was expected, the flux of nitrite towards the bulk liquid and towards the anammox zone increased when the DO concentration in the bulk liquid increased.

4.3.3. *Anammox zone*

In order to obtain the maximal anammox activity inside the granule, neither ammonium nor nitrite concentrations should be limiting. Therefore, high concentrations of ammonium (initial concentration of 140 mg NH_4^+–N L^{-1}) and nitrite (from 8.4 to 42.0 mg NO_2^-–N L^{-1}) were applied in the bulk liquid while the DO concentration was kept at air saturation (8 mg O_2 L^{-1}). The CANON reactors are normally operated under nitrite limitation since it is necessary to keep the anammox potential higher than the nitrification potential in order to avoid the occurrence of nitrite build-up which is usually followed by irreversible nitrite inhibition of the anammox biomass (Nielsen et al., 2005).

Even in those experiments performed with pure oxygen saturation, the NO_2^- concentration in the bulk liquid of 1.3 mg N L^{-1} was not sufficient to attain maximal anammox activity since NO_2^- concentration became zero in the deeper layers where anammox bacteria were still present. The strategy followed to estimate the maximal anammox activity was to maintain the DO concentration at 8 mg O_2 L^{-1} (the conditions of the granular SBR) and to increase the NO_2^- concentration in the bulk liquid. In the experiment carried out at a nitrite concentration in the bulk liquid of 9 mg N L^{-1} (Fig. 6), the nitrite concentration obtained in the inner core of the granule was 0.7 mg N L^{-1}. Since nitrite half saturation constant of anammox bacteria was reported to be less than 0.1 mg N L^{-1} (Strous et al., 1999), maximal anammox activity in the granule was then ensured.

From the nitrite profiles obtained in Fig. 5 and Fig. 6 it can be inferred that, by keeping the DO concentration in the bulk liquid constant, the increase of the NO_2^- concentration in the bulk liquid increases the flux of nitrite to the anammox zone up to a maximum value of 1.0 g N m^{-2} d^{-1} (Table 3). Such high fluxes of nitrite to the anoxic layers of the granule are expected during the SBR operation since the mean nitrite concentration in the bulk liquid ranged between 12 and 42 mg N L^{-1}.

Kindaichi et al. (2007) obtained a similar maximal nitrite removal capacity with a maximal volumetric rate of 5.0 g N $(L_{biofilm})^{-1}$ d^{-1} and a similar NO_2^- flux of 2.2 g N m^{-2} d^{-1} performing microprofiles in the biofilm of an anaerobic fixed bed column operated at 37 °C. However in their case, the maximal anammox reaction width was over 1300 μm of the biofilm, whereas in the present study, anammox bacteria were located in the range of depths between 400 and 1000 μm.

Using the information of the NO_2^- microprofiles, an estimation of the nitrogen removal rate of the SBR using Eq. 12 was performed. With these data and taking into account the stoichiometry of the anammox reaction, an ANR of 0.5 g N L^{-1} d^{-1} was estimated in the SBR. This value was close to the mean ANR value obtained in the reactor from the macroscopic measurements (Fig. 1). Our microscopic analysis of the granules was thus in agreement with macroscopic observations.

4.3.4. *Causes of error*

In order to better explain the obtained results, the different assumptions made during the performance of the experiments with the microsensors and the corresponding calculations have to be analyzed. As it was indicated the calculations were based on the assumption that the granules are described as flat surfaces, whereas the granules were sphere shaped and thus this fact could influence the flow pattern. Besides, it was assumed that the granules were homogeneous in structure. It has been widely demonstrated that biofilms are heterogeneous and therefore diffusivities should be locally defined. However, it was beyond the scope of this article to study in depth the heterogeneity of the bacteria populations and the approximations done are satisfactory to give important information about the processes carried out into the granule. Finally, the surface layer of the granule was somewhat fluffy, where a visual definition of "surface" within ±50 μm was difficult. By performing several repetitions, the high values obtained for the standard deviations confirmed the high variability of the results, but, as it will be further explained, the approximations were satisfactory since the microscopic results predicted to a high extent the macroscopic ones.

4.4. *From microscale results to granular CANON operation*

A successful strategy to start-up a CANON reactor is the promotion of the growth of the AOB population in the form of granular biomass. AOB produce nitrite and consume oxygen to provide anoxic conditions in the inner core of the granules. In this anoxic zone, ammonium (left from the AOB activity) and nitrite (from partial nitrification) have to be present in order to allow the growth of anammox bacteria (Vázquez-Padín et al.,

Table 3 – DO and NO^- fluxes in and out of the nitrifying zone at different DO concentrations in the bulk liquid. The NO^- concentration in the bulk liquid was kept at about 1 mg N L^{-1}.

DO_{bulk} (mg O_2 L^{-1})	$J_{O_2}^{DBL}$ (g O_2 m^{-2} d^{-1})	$J_{NO_2}^{Total} = J_{NO_2}^{DBL} + J_{NO_2}^{Amx}$ (g N m^{-2} d^{-1})	$J_{NO_2}^{Amx}$ (g N m^{-2} d^{-1})	$J_{O_2}^{DBL}(J_{NO_2}^{Total})^{-1}$ (g O_2 (g N)$^{-1}$)
35.2	20.2	2.7	1.0	7.5
20.5	11.9	2.3	0.7	5.2
8.1	5.1	1.3	0.4	4.0

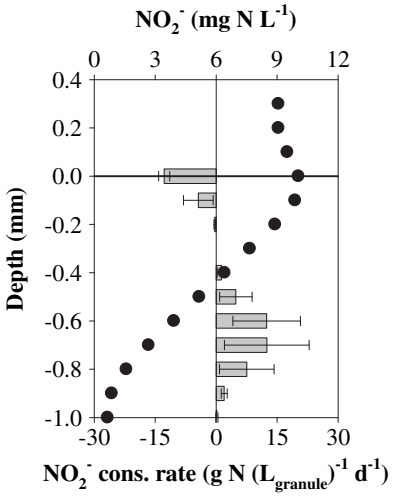

Fig. 6 – Nitrite concentration profile (●) and average local consumption rate (▫; bars indicate standard deviation: $n = 6$) by incubation with a NO_2^- concentration of 9 mg N L^{-1} in the bulk liquid.

2009). The width of the external layer mainly composed by AOB should be thick enough to protect anammox bacteria from the penetration of dissolved oxygen, but its activity must be controlled to avoid inhibition of anammox bacteria by high nitrite concentrations. From the results obtained by application of microsensors it is possible to extract knowledge about both optimal and safe conditions for the operation of the CANON system, in terms of ammonia and nitrite concentrations in the bulk liquid. At this point a control strategy could be defined to regulate the concentration of both compounds by using on-line ammonia and nitrite analyzers. The variables of control would be the DO concentration and the HRT value using the air flow rate and the inlet flow rate as actuation elements.

Different scenarios for the different ranges of ammonium and nitrite concentrations are possible (Fig. 7a). Low NH_4^+ and NO_2^- concentrations would limit the activities of AOB and/or anammox bacteria. AOB activity would be limited by the ammonia concentration when the ratio DO/NH_4^+ (R_{ON}) in the bulk liquid is lower than 3.4 g O_2 (g N)$^{-1}$ D_{NH4}/D_{O2} (Harremoes and Henze, 2002). The limitation of AOB by ammonia would expose the reactor to a risk of failure since the granules would be fully penetrated by oxygen which would temporally inhibit anammox bacteria and enhance the undesired growth of NOB (Sliekers et al., 2005). On the other hand, high NH_4^+ and/or NO_2^- concentrations have the following disadvantages: both substrates can inhibit AOB and anammox bacteria with a consequent detriment of the produced effluent quality. Moreover, maintaining concentrations of NO_2^- higher than the optimal ones involves higher costs of aeration.

The control strategy corresponding to the different defined zones to restore the optimal conditions will be: a) in case of nitrite concentration out of the optimal range to act over the DO concentration (increasing or decreasing its value); b) whereas to optimize the NH_4^+ concentration the value of the HRT must be modified as the control parameter; and in the case where NH_4^+ and NO_2^- concentrations were not in the optimal range, both, HRT value and DO concentration would be changed according to Fig. 7b.

Making use of the previous qualitative analysis the optimal values for NH_4^+ and NO_2^- concentrations can be defined for a specific case. These parameters will be determined specifically for the biomass present in each CANON reactor.

From the microprofiles measured into the granules, the minimum nitrite concentration required to avoid substrate limitation for anammox bacteria can be estimated. Then, from these values and taking into account the stoichiometry of the partial nitrification and anammox processes, a minimum ammonium concentration in the bulk liquid can also be calculated. The fact that a minimal concentration of both ammonium and nitrite are necessary in the bulk liquid to

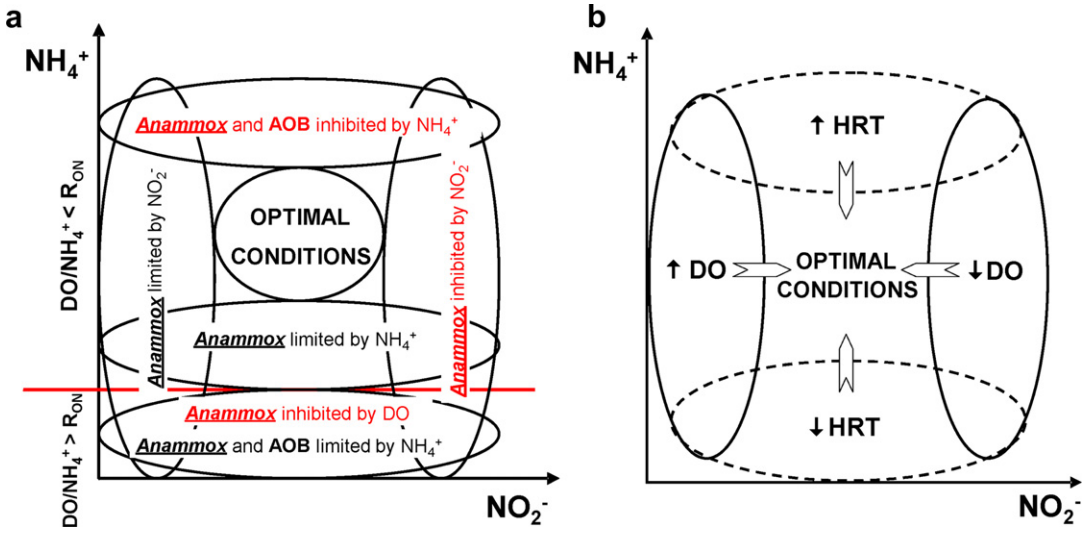

Fig. 7 – a) Zones defining the different operational conditions in a CANON reactor fed with different NH_4^+ and NO_2^- concentrations in the bulk liquid. b) Control strategy to return the CANON reactor to optimal conditions depending on NH_4^+ and NO_2^- concentrations in the bulk liquid. ($R_{ON} = 3.4\ D_{NH_4}/D_{O_2}$).

ensure the maximal activity of anammox bacteria can represent a drawback if the effluent of the CANON reactor has to be released to a natural media but has not a significant impact if the effluent is returned to the head of the WWTP.

5. Conclusions

- Ammonia oxidation to nitrite is highly dependent on the oxygen mass transfer. Oxygen limitation regulates the amount of nitrite produced and as a consequence influences the anammox activity. Nitrite microprofiles revealed that a minimum nitrite concentration around 9 mg N L^{-1} was necessary to ensure that the anammox biomass was working at maximal activity.
- Oxygen and nitrite microprofiles determined by application of microsensors correlated to the distributions of AOB and anammox bacteria inside the granules.
- Estimated bacterial activities from microscale analysis (0.5 g N L^{-1} d^{-1}) gave similar results to those obtained from macroscopic measurements in the granular SBR.
- Accurate regulation of the dissolved oxygen concentration in the bulk liquid and the HRT value are crucial to control the nitrogen removal process in a CANON system avoiding either limitations or inhibitory phenomena.

Acknowledgement

This work was funded by the Spanish Government (Togransys and NOVEDAR_Consolider project CSD2007-00055). We gratefully acknowledge Preben Sorensen for technical assistance, Andreas Schramm and Daniel Aagren Nielsen for assistance with cryosectioning and FISH.

REFERENCES

Amann, R., Ludwig, W., Schleifer, K.H., 1995. Phylogenetic identification and in-situ detection of individual microbial-cells without cultivation. Microbiological Reviews 59 (1), 143–169.

Beun, J.J., Heijnen, J.J., van Loosdrecht, M.C.M., 2001. N-removal in a granular sludge sequencing batch airlift reactor. Biotechnology and Bioengineering 75 (1), 82–92.

Crocetti, G.R., Banfield, J.F., Keller, J., Bond, P.L., Blackall, L.L., 2002. Glycogen-accumulating organisms in laboratory-scale and full-scale wastewater treatment processes. Microbiology 148 (11), 3353–3364.

Dapena-Mora, A., Fernandez, I., Campos, J.L., Mosquera-Corral, A. , Mendez, R., Jetten, M.S.M., 2007. Evaluation of activity and inhibition effects on anammox process by batch tests based on the nitrogen gas production. Enzyme and Microbial Technology 40 (4), 859–865.

de Beer, D., van den Heuvel, J.C., Ottengraf, S.P.P., 1993. Microelectrode measurements of the activity distribution in nitrifying bacterial aggregates. Applied and Environmental Microbiology 59 (2), 573–579.

Dosta, J., Fernandez, I., Vazquez-Padin, J.R., Mosquera-Corral, A., Campos, J.L., Mata-Alvarez, J., Mendez, R., 2008. Short- and long-term effects of temperature on the anammox process. Journal of Hazardous Materials 154 (1–3), 688–693.

Freitag, T.E., Prosser, J.I., 2003. Community structure of ammonia-oxidizing bacteria within anoxic marine sediments. Applied and Environmental Microbiology 69 (3), 1359–1371.

Gieseke, A., Bjerrum, L., Wagner, M., Amann, R., 2003. Structure and activity of multiple nitrifying bacterial populations co-existing in a biofilm. Environmental Microbiology 5 (5), 355–369.

Gieseke, A., Tarre, S., Green, M., de Beer, D., 2006. Nitrification in a biofilm at low pH values: role of in situ microenvironments and acid tolerance. Applied and Environmental Microbiology 72 (6), 4283–4292.

Guisasola, A., Jubany, I., Baeza, J.A., Carrera, J., Lafuente, J., 2005. Respirometric estimation of the oxygen affinity constants for biological ammonium and nitrite oxidation. Journal of Chemical Technology and Biotechnology 80 (4), 388–396.

Harremoes, P., Henze, M., 2002. Wastewater Treatment. In: Henze, M., Harremoes, P., La Cour Jansen, J., Arvin, E. (Eds.). Springer, pp. 157–208.

Hippen, A., Rosenwinkel, K.H., Baumgarten, G., Seyfried, C.F., 1997. Aerobic deammonification: a new experience in the treatment of wastewaters. Water Science and Technology 35 (10), 111–120.

Jørgensen, B.B., Revsbech, N.P., 1985. Diffusive boundary layers and the oxygen uptake of sediments and detritus. Limnology and Oceanography 30, 11–21.

Jubany, I., Carrera, J., Lafuente, J., Baeza, J.A., 2008. Start-up of a nitrification system with automatic control to treat highly concentrated ammonium wastewater: experimental results and modeling. Chemical Engineering Journal 144 (3), 407–419.

Kindaichi, T., Kawano, Y., Ito, T., Satoh, H., Okabe, S., 2006. Population dynamics and in situ kinetics of nitrifying bacteria in autotrophic nitrifying biofilms as determined by real-time quantitative PCR. Biotechnology and Bioengineering 94 (6), 1111–1121.

Kindaichi, T., Tsushima, I., Ogasawara, Y., Shimokawa, M., Ozaki, N., Satoh, H., Okabe, S., 2007. In situ activity and spatial organization of anaerobic ammonium-oxidizing (anammox) bacteria in biofilms. Applied and Environmental Microbiology 73 (15), 4931–4939.

Kjær, T., Larsen, L.H., Revsbech, N.P., 1999. Sensitivity control of ion-selective biosensors by electrophoretically mediated analyte transport. Analytica chimica acta 391 (1), 57–63.

Kuai, L.P., Verstraete, W., 1998. Ammonium removal by the oxygen-limited autotrophic nitrification-denitrification system. Applied and Environmental Microbiology 64 (11), 4500–4506.

Li, Y.H., Gregory, S., 1974. Diffusion of ions in sea-water and in deep-sea sediments. Geochimica et Cosmochimica Acta 38 (5), 703–714.

Lorenzen, J., Larsen, L.H., Kjaer, T., Revsbech, N.P., 1998. Biosensor determination of the microscale distribution of nitrate, nitrate assimilation, nitrification, and denitrification in a diatom-inhabited freshwater sediment. Applied and Environmental Microbiology 64 (9), 3264–3269.

Loy, A., Maixner, F., Wagner, M., Horn, M., 2007. probeBase – an online resource for rRNA-targeted oligonucleotide probes: new features 2007. Nucleic Acids Research 35 (Suppl. 1), D800–D804.

Mosquera-Corral, A., Gonzalez, F., Campos, J.L., Mendez, R., 2005. Partial nitrification in a SHARON reactor in the presence of salts and organic carbon compounds. Process Biochemistry 40 (9), 3109–3118.

Nielsen, M., Bollmann, A., Sliekers, O., Jetten, M., Schmid, M., Strous, M., Schmidt, I., Larsen, L.H., Nielsen, L.P., Revsbech, N. P., 2005. Kinetics, diffusional limitation and microscale distribution of chemistry and organisms in a CANON reactor. FEMS Microbiology Ecology 51 (2), 247–256.

Okabe, S., Satoh, H., Watanabe, Y., 1999. In situ analysis of nitrifying biofilms as determined by in situ hybridization and

the use of microelectrodes. Applied and Environmental Microbiology 65 (7), 3182–3191.
Picioreanu, C., van Loosdrecht, M.C.M., Heijnen, J.J., 1997. Modelling the effect of oxygen concentration on nitrite accumulation in a biofilm airlift suspension reactor. Water Science and Technology 36 (1), 147–156.
Ploug, H., Kuhl, M., BuchholzCleven, B., Jorgensen, B.B., 1997. Anoxic aggregates – an ephemeral phenomenon in the pelagic environment? Aquatic Microbial Ecology 13 (3), 285–294.
Rasmussen, K., Lewandowski, Z., 1998. Microelectrode measurements of local mass transport rates in heterogeneous biofilms. Biotechnology and Bioengineering 59 (3), 302–309.
Reimer, M., Harremoes, P., 1978. Multi-component diffusion in denitrifying biofilm. Progress in Water Technology 10, 149–165.
Revsbech, N.P., 1989. An oxygen microsensor with a guard cathode. Limnology and Oceanography 34 (2), 474–478.
Schramm, A., de Beer, D., Wagner, M., Amann, R., 1998. Identification and activities in situ of *Nitrosospira* and *Nitrospira* spp. as dominant populations in a nitrifying fluidized bed reactor. Applied and Environmental Microbiology 64 (9), 3480–3485.
Schramm, A., de Beer, D., van den Heuvel, J.C., Ottengraf, S., Amann, R., 1999. Microscale distribution of populations and activities of *Nitrosospira* and *Nitrospira* spp. along a macroscale gradient in a nitrifying bioreactor: quantification by in situ hybridization and the use of microsensors. Applied and Environmental Microbiology 65 (8), 3690–3696.
Sliekers, A.O., Haaijer, S.C.M., Stafsnes, M.H., Kuenen, J.G., Jetten, M.S.M., 2005. Competition and coexistence of aerobic ammonium- and nitrite-oxidizing bacteria at low oxygen concentrations. Applied Microbiology and Biotechnology 68 (6), 808–817.
Strous, M., VanGerven, E., Zheng, P., Kuenen, J.G., Jetten, M.S.M., 1997. Ammonium removal from concentrated waste streams with the anaerobic ammonium oxidation (anammox) process in different reactor configurations. Water Research 31 (8), 1955–1962.
Strous, M., Kuenen, J.G., Jetten, M.S.M., 1999. Key physiology of anaerobic ammonium oxidation. Applied and Environmental Microbiology 65 (7), 3248–3250.
Third, K.A., Sliekers, A.O., Kuenen, J.G., Jetten, M.S.M., 2001. The CANON system (completely autotrophic nitrogen-removal over nitrite) under ammonium limitation: Interaction and competition between three groups of bacteria. Systematic and Applied Microbiology 24 (4), 588–596.
van Dongen, U., Jetten, M.S.M., van Loosdrecht, M.C.M., 2001. The SHARON®-Anammox® process for treatment of ammonium rich wastewater. Water Science and Technology 44 (1), 153–160.
Vázquez-Padín, J.R., Fernández, I., Figueroa, M., Mosquera-Corral, A., Campos, J.L., Méndez, R., 2009. Applications of anammox based processes to treat anaerobic digester supernatant at room temperature. Bioresource Technology 100, 2988–2994.
Vlaeminck, S.E., Cloetens, L.F.F., Carballa, M., Boon, N., Verstraete, W., 2008. Granular biomass capable of partial nitritation and anammox. Water Science and Technology 58 (5), 1113–1120.
Wiesmann, U., 1994. Advances in Biochemical Engineering/ Biotechnology, Heidelberg, pp. 113–154.
Wilen, B.M., Gapes, D., Keller, J., 2004. Determination of external and internal mass transfer limitation in nitrifying microbial aggregates. Biotechnology and Bioengineering 86 (4), 445–457.
Wilhelm, R., Abeliovich, A., Nejidat, A., 1998. Effect of long-term ammonia starvation on the oxidation of ammonia and hydroxylamine by *Nitrosomonas europaea*. Journal of Biochemistry 124 (4), 811–815.